doi: 10.4149/gpb_2024015

LncRNA SNHG1 knockdown attenuates lipopolysaccharide-induced acute lung injury *via* regulating miR199a-3p/ROCK2 axis

Wei Qian[1,*], Yan Han[2,*], Yan Jin[3], Changjiang Lei[4] and Xue Lin[3]

[1] *Department of Radiology, The Fifth Hospital of Wuhan, Wuhan, China*
[2] *Department of General Medicine, Qin Duankou Street Community Health Service Center Affiliated to The Fifth Hospital of Wuhan, Wuhan, China*
[3] *Department of Emergency, The Second Hospital of Dalian Medical University, Liaoning, China*
[4] *Department of Oncology, The Fifth Hospital of Wuhan, Wuhan, China*

Abstract. Acute lung injury (ALI) is a significant health condition with notable rates of morbidity and mortality globally. Long non-coding ribose nucleic acids (lncRNAs) play vital roles in mitigating various inflammation-related diseases, including ALI. The study aimed to investigate the functional role and molecular mechanisms of lncRNA SNHG1 on ALI in lipopolysaccharide (LPS)-treated A549 cells and in LPS-induced ALI mice. The expression of SNHG1 was initially examined in LPS-treated A549 cells. We further demonstrated the critical function of SNHG1 through various cellular assessments following SNHG1 knockdown, including cell counting kit (CCK)-8 assay, flow cytometry analysis, as well as enzyme-linked immunosorbent assay (ELISA). Reducing SNHG1 levels hindered the negative effects of LPS on cell viability, apoptosis, and inflammation. Moreover, SNHG1 acted as a negative regulator for miR-199a-3p, which targeted downstream ROCK2. Depletion of miR-199a-3p or enhanced expression of ROCK2 abolished the protective effects of SNHG1 knockdown on LPS-induced apoptosis and inflammation. Consistently, silencing SNHG1 alleviated LPS-induced lung injury in mice, demonstrating its potential therapeutic benefits in managing ALI. Overall, this study sheds light on the role of SNHG1 in modulating inflammation and apoptosis in ALI through the miR-199a-3p/ROCK2 pathway, offering new insights for the treatment of this condition.

Key words: Acute lung injury — Lipopolysaccharide — SNHG1 — miR-199a-3p — ROCK2

Introduction

Acute lung injury (ALI) is a serious condition associated with high morbidity and mortality rates, characterized by diffuse alveolar damage (DAD), inflammatory responses, neutrophil recruitment, and cell apoptosis (Mowery et al. 2020). The pathophysiology of ALI is intricate and encompasses multiple mechanisms such as inflammatory responses, lung oxidative stress, and cellular apoptosis or necrosis (Wang et al. 2018). Current treatment options for ALI are primarily

* These authors contributed equally to this work.
Correspondence to: Chanjiang Lei, Department of Oncology, The Fifth Hospital of Wuhan, 122 Xianzheng Streat, Hanyang District, Wuhan, Hubei 430050, China
E-mail: 305069071@qq.com
Xue Lin, Department of Emergency, The Second Hospital of Dalian Medical University, No. 467, Zhongshan Road, Shahekou District, Dalian City, Liaoning 116000, PR China
E-mail: hutew547@163.com

© The Authors 2024. This is an **open access** article under the terms of the Creative Commons Attribution-NonCommercial 4.0 International License (https://creativecommons.org/licenses/by-nc/4.0/), which permits non-commercial use, distribution, and reproduction in any medium, provided the original work is properly cited.

limited to supportive therapies, indicating a critical need for the development of more targeted and efficient therapeutic strategies (Schmidt 2016). It is imperative to delve deeper into the pathogenesis of ALI to identify systemic and highly effective treatment approaches to significantly improve patient outcomes

Long non-coding RNAs (lncRNAs), a class of non-coding RNAs with lengths exceeding 200 nucleotides, have been implicated in a wide range of biological processes, including cell cycle regulation, differentiation, mRNA alternative splicing, and translation (Mercer et al. 2009; Fatica et al. 2014). The potential regulatory roles of lncRNAs in the development of ALI have garnered increasing attention from researchers aiming to unravel the underlying pathophysiological mechanisms and identify novel therapeutic targets. For instance, a study demonstrated that lipopolysaccharide (LPS)-induced ALI mice and mouse alveolar macrophage (MHS) cells exhibited elevated levels of Nuclear Paraspeckle Assembly Transcript 1 (NEAT1), and the knockdown of NEAT1 attenuated LPS-induced inflammation and apoptosis *via* the miR-182-5p/Wingless-Type MMTV Integration Site Family Member 1 (WNT1)-inducible-signaling pathway protein 1 (WISP1) axis (Lv et al. 2021). Another study revealed that lncRNA derived from Taurine Upregulated Gene 1 (TUG1) exerted protective effects on LPS-stimulated pulmonary microvascular endothelial cells (PMVECs) by reducing inflammation and apoptosis through the modulation of miR-34b-5p and growth factor receptor-bound protein 2-associated binding protein 1 (GAB1) (Qiu et al. 2020).

Small nucleolar RNA host gene 1 (SNHG1) is a recently discovered lncRNA situated on chromosome 11q12.3. It has been shown to play a crucial role in the pathogenesis of several cancers, such as gastric cancer, hepatocellular carcinoma, bladder cancer, and glioma (Li et al. 2019; Liu et al. 2019; Liu et al. 2020; Xu et al. 2020). While SNHG1 has been significantly implicated in the regulation of macrophage inflammatory activation through targeting HMGB1 axis (Hu et al. 2022), its exact role and underlying mechanisms in the context of ALI remain to be fully elucidated.

MicroRNAs (miRNAs) are a group of non-coding RNAs that play pivotal roles in various biological processes, such as inflammation, apoptosis, immunity, and cell differentiation, by modulating the expression of protein-coding genes (Gantier 2010). In the context of ALI, several miRNAs have been found to be differentially expressed (Cai et al. 2012). Among them, miR-199a displays acute down-regulation in sepsis-induced ALC (Cai et al. 2012; Liu et al. 2018). Moreover, a recent study reported that miR-199a-3p-enriched bone marrow mesenchymal stem cell exosomes (BMSC-exo) modulated the epithelial sodium channel (ENaC), thereby exhibiting anti-inflammatory effects in ALI (Chen L et al. 2022). Additionally, Rho-associated coiled-coil containing protein kinase 2 (ROCK2), a serine-threonine kinase that is activated under stress conditions, has been found to be upregulated in ALI (Chen H et al. 2020; Ren et al. 2022). Intriguingly, bioinformatic analyses suggest that SNHG1 could potentially interact with miR-199a-3p and that ROCK2 might be one of the downstream targets of miR-199a-3p.

In light of these considerations, this study aimed to elucidate the effects of SNHG1 and the miR-199a-3p/ROCK2 axis in ALI. We investigated the role and molecular mechanisms of lncRNA SNHG1 in ALI using *in vitro* LPS-treated A549 cells and an *in vivo* LPS-induced ALI mouse model. We found that SNHG1 knockdown attenuated LPS-induced inflammation and apoptosis in A549 cells, and this effect was mediated through the miR-199a-3p/ROCK2 axis. Collectively, our findings provide novel insights into the potential therapeutic targets for ALI and may contribute to the development of new treatment strategies.

Materials and Methods

Cell culture and transfection

Human adenocarcinoma alveolar basal epithelial cells (A549 cell line) were purchased from the American Type Culture Collection (ATCC, Manassas, USA). The cells were cultured in the Roswell Park Memorial Institute (RPMI)-1640 medium (Gibco, Grand Island, USA) supplemented with 10% fetal bovine serum (FBS, Gibco) in a humidified atmosphere with 5% CO_2 at 37°C. The siRNAs targeting SNHG1, miR-199a-3p mimics, and miR-199a-3p inhibitors were synthesized by GenePharma Co., Ltd. (Shanghai, China). ROCK2 cDNA was cloned into pcDNA3.1 vector to overexpress ROCK2 (Sangon Biotech Co., Ltd., Shanghai, China). The cell transfection was conducted using lipofectamine® 2000 (Invitrogen, Carlsbad, USA) according to the manufacturer's instructions.

RT-qPCR analysis

Total RNA samples from cells (1×10^6) or tissues (10 mg) were initially extracted using the TRIzol reagent (Invitrogen, Waltham, USA). Then, 1 μg of RNA sample was reverse transcribed into complementary deoxyribose nucleic acid (cDNA) using HiScript III 1st Strand cDNA Synthesis Kit (Vazyme Biotech Co. Ltd., Nanjing, China) following the manufacturer's instructions. Further, the cDNA amplification was conducted with Universal SYBR qPCR Master Mix (Vazyme Biotech Co. Ltd.). Glyceraldehyde 3-phosphate dehydrogenase (GAPDH) was used as an internal control for the mRNA and lncRNA, and snRNA U6 was employed

for miR-199a-3p normalization. The sequences of used Primers are in Table 1.

CCK-8 and LDH assays

The cell proliferation ability was determined using the CCK-8 assay. Initially, A549 cells were transfected with indicated siRNA or miRNA mimics. The harvested single-cell suspensions were prepared and seeded into the 96-well plate (2500 cells/well) within the volume of 100 µl *per* well. After incubation at 37°C in a 5% CO_2 incubator for required time intervals, 10 µl of CCK-8 reagent (Beyotime Biotechnology, China) was added at 24, 48, and 72 h. After an additional 4 h incubation, optical density (OD) values at 450 nm were recorded with a microplate reader (Molecular Devices, Silicon Valley, USA). For LDH assay, cells samples after transfection were seeded at a density of 5000 cells/well in the 96-well plate for 48 h. The cell culture media were collected for LDH activity detection using Cytotox 96 non-radioactive cytotoxicity assay (Promega, Madison, USA), as *per* the manufacturer's instructions.

Western blot analysis

The cell lysate was harvested using the radioimmunoprecipitation assay (RIPA) buffer with phenylmethylsulfonyl fluoride (PMSF) and a protein inhibitor cocktail. Following centrifugation, the protein concentration was accurately measured with a bicinchoninic acid (BCA) assay reagent kit (Beyotime Biotechnology Co. Ltd., Shanghai, China). Subsequently, 20–40 µg of protein was loaded onto a sodium dodecyl sulfate-polyacrylamide gel electrophoresis (SDS-PAGE) and transferred to a polyvinylidene difluoride (PVDF) membrane. The membrane was then blocked with 5% skimmed milk and probed with specific primary antibodies, such as anti-Bcl2, anti-caspase-3, anti-ROCK2, and anti-GAPDH (Cell signaling technology, 15071, 9662, 47012, and 5174, Danvers USA) overnight at 4°C. Following washing with tris-buffered saline-Tween 20 (TBS), the membranes were incubated with horseradish peroxidase (HRP)-conjugated secondary antibodies. Finally, the blots were visualized using a chemiluminescence system.

ELISA

Following the treatment of selected cell lines and animals, the production of different cytokines and their concentrations were assessed using corresponding ELISA kits. The expression levels of various inflammatory factors such as tumor necrosis factor α (TNF)-α, interleukin (IL)-1β, and IL-6 in the supernatant from A549 cell culture media and bronchoalveolar lavage fluid (BALF) were measured using commercial ELISA kits from R&D, Minneapolis, USA, following the manufacturer's instructions. Subsequently, the obtained readings were analyzed using a microplate reader.

Table 1. Primer sequences

Gene	Primer	Sequence
GAPDH	F	GGAGCGAGATCCCTCCAAAAT
	R	GGCTGTTGTCATACTTCTCATGG
SNHG1	F	ACAGCAGTTGAGGGTTTGCT
	R	GGCTCATGACGGGAACAGAA
ROCK2	F	TGATTGGTGGTCTGTAGG
	R	GCTGCCGTTTCTCTTATG
U6	F	ATTGGAACGATACAGAGAAGATT
	R	GGAACGCTTCACGAATTTG
miR-199a-3p	F	GCGCGACAGTAGTCTGCACAT
	R	AGTGCAGGGTCCGAGGTATT

F, forward; R, reverse.

Fluorescence-activated cell sorting (FACS) analysis

The apoptosis assay for cells was carried out by utilizing the Annexin V-Fluorescein isothiocyanate (FITC) Apoptosis Detection Kit from BD Pharmingen in San Diego, USA, as *per* the instructions provided by the manufacturer. After the treatment or transfection, the cells were harvested and washed with phosphate-buffered saline (PBS). Next, the cells were stained with Annexin V-FITC and propidium iodide (PI) for a duration of 15 min. Following this, the samples were examined using flow cytometry equipment from BD Biosciences in CA, USA.

Dual-luciferase reporter assay

The wild-type sequences of SHNG1 and ROCK2 mRNA 3' UTR, which contain the miR-199a-3p binding sites, and mutant versions of SHNG1 and ROCK2 3'UTR with mutations in the conserved binding sites, were synthesized and inserted into the pmirGLO luciferase vector. These vectors were then transfected into A549 cells with either negative control (NC) mimics or miR-199a-3p mimics. After 48 h, the cells were harvested, and luciferase activity was measured using the Dual-Luciferase Reporter System (Promega, Madison, USA) to assess firefly (Photinus pyralis) and sea pansy (Renilla reniformis) luciferase levels.

RNA immunoprecipitation (RIP) and RNA pulldown assays

The EZ Magna RNA immunoprecipitation Kit (Millipore, Burlington, USA) was utilized for the anti-Ago2 RIP assay following the manufacturer's guidelines. A549 cell lysate was collected and incubated with Magnetic beads conjugated with an Ago2 antibody (Abcam, Cambridge, MA)

or immunoglobulin G (IgG control) at 4°C overnight. Post bead washing, RNA was extracted using TRIzol reagent and subjected to RT-qPCR analysis. RNA pulldown assay was conducted using the Magnetic RNA Protein Pull-Down Kit (Pierce Manufacturing, Appleton, USA) as *per* the manufacturer's instructions. Biotin-labeled miR-119a-3p mimic or NC was transfected into A549 cells for 48 h. The cell lysate was collected and incubated with streptavidin-conjugated magnetic beads. Precipitated RNA from the beads or input RNA samples were extracted using TRIzol reagent. Subsequently, the relative enrichment of SNHG1 was assessed by RT-qPCR.

In vivo investigations

C57BL/6 mice (n = 32) were procured from the Shanghai Laboratory Animal Center, Chinese Academy of Sciences (CAS, Shanghai, China). Approval for all animal-related experiments and procedures was obtained from the Animal Policy and Welfare Committee of the Second Hospital of Dalian Medical University. The mice were divided into four groups: vehicle control (con), LPS-induced ALI group (LPS), negative control group – the adeno-associated virus (LPS+AAV-NC), and SNHG1 silence of LPS-induced ALI (LPS+shAAV-SHNG1) (n = 8 *per* group). The ALI injury model was induced in the respective groups by intraperitoneal injection of LPS (2 mg/kg of body weight) or control PBS. Prior to LPS induction, mice in the negative control or SHNG1 silence treatment groups received intravenous injections of shAAV-NC or shAAV-SHNG1, respectively, 24 h in advance. One week after LPS administration, anesthesia was administered using pentobarbital sodium (50 mg/kg) and all mice were euthanized by cervical dislocation for lung tissue collection.

H&E staining

The right lung tissues were collected from euthanized mice, washed with PBS, fixed in 4% formaldehyde, and embedded in paraffin. Subsequently, the lung tissues were sectioned into 4 μm thick sections and mounted on glass slides. Following deparaffinization and rehydration in xylene and ethanol, the tissue sections underwent antigen retrieval by microwave treatment and were stained with hematoxylin and eosin (H&E staining kit, Beyotime, Beijing, China) for histopathological analysis. Finally, the stained cells were examined under a light microscope (Carl Zeiss, Jena, Germany).

TdT-mediated dUTP nick end labeling (TUNEL) assay

The TUNEL assay was conducted using the *in situ*, Cell Death Detection Kit (Roche, Penzberg, Germany) following the provided guidelines. Initially, slides with tissue sections were deparaffinized and washed with PBS, then permeabilized with 0.1% Triton X-100 and 0.1% sodium citrate at 41°C for 2 min. Subsequently, the slides were exposed to a TUNEL reaction buffer containing TdT- and FITC-labeled dUTP at 37°C for 1 h in the absence of light. Following rinsing, the tissue slides were mounted using an antifade solution, and images were captured with a FITC (TUNEL) filter. The percentage of apoptotic cells in the tissue sections was determined through morphometric analysis of 10 cross-sections from each experimental group, using Image Analysis Software from Olympus Italia (Segrate, Italy).

Statistical analysis

Data were presented as mean ± standard deviation (S.D.). The GraphPad Prism 7.0 software (La Jolla, USA) was used for statistical analysis. The differences between groups were evaluated by Student's t-test for two groups and analysis of variance (ANOVA) for multiple groups, considering $p < 0.05$ statistically significant.

Results

SNHG1 knockdown attenuates LPS-induced cell injury in A549 cells

The expression level of SNHG1 mRNA was initially compared in A549 cells with or without LPS stimulation. RT-qPCR results revealed an increase in SNHG1 mRNA levels following LPS stimulation (Fig. 1A). To further investigate the role of SNHG1, three small interfering RNAs (siRNAs) – si-SNHG1#1, si-SNHG1#2, and si-SNHG1#3 – were utilized to deplete SNHG1. Evaluation of the knockdown effect by RT-qPCR indicated that siSNHG1#1 exhibited the most significant knockdown efficiency among the tested siRNAs (Fig. 1B), prompting its selection for subsequent experiments. Subsequent CCK-8 and LDH assays demonstrated that LPS treatment led to a notable decrease in the proliferation of A549 cells and an increase in cell death. Interestingly, SNHG1 knockdown effectively mitigated the adverse effects of LPS treatment (Fig. 1C,D). Additionally, flow cytometry analysis revealed a higher proportion of apoptotic cells following LPS induction, which was partially reversed by SNHG1 knockdown in A549 cells (Fig. 1E). Western blot analysis confirmed alterations in the expression levels of apoptosis-related proteins post-LPS stimulation, with increased cleaved caspase-3 and decreased Bcl-2 levels. Notably, SNHG1 silencing restored Bcl-2 expression and downregulated cleaved caspase-3 levels (Fig. 1F). ELISA results showed a significant increase in TNF-α, IL-1β, and

IL-6 secretion upon LPS stimulation, whereas SNHG1 siRNA treatment effectively suppressed the upregulation of these proinflammatory cytokines in A549 cells (Fig. 1G). These findings collectively suggest that SNHG1 downregulation exerts substantial anti-apoptotic and anti-inflammatory effects in A549 cells.

SNHG1 acts as a regulator for miR-199a-3p in A549 cells

To further elucidate the molecular mechanistic role of SNHG1 in LPS-induced inflammation and apoptosis, we conducted a comprehensive search of SNHG1 target miRNAs using the StarBase database. Our investigation revealed a potential binding interaction between SNHG1 and miR-199a-3p (Fig. 2A). Subsequent luciferase assays demonstrated that miR-199a-3p mimic specifically inhibited the activity of wild-type SNHG1 reporter, not the mutant version report, in A549 cells (Fig. 2B). Furthermore, RNA pulldown assay confirmed the enrichment of endogenous SNHG1 by biotinylated miR-199a-3p-transfected A549 cells compared to the biotinylated-NC sample group, indicating a direct interaction between SNHG1 and miR-199a-3p (Fig. 2C). Additionally, results from RIP assays showed the enrichment of SNHG1 and miR-199a-3p in Ago2-containing micro-ribonucleoprotein complexes, suggesting the functional association of SNHG1 and miR-199a-3p with Ago2 protein (Fig. 2D). Interestingly, treatment with LPS led to a decrease in miR-199a-3p levels, while silencing SNHG1 resulted in an upregulation of miR-199a-3p expression in A549 cells (Fig. 2E,F). These findings indicate that miR-199a-3p is a downstream target of SNHG1.

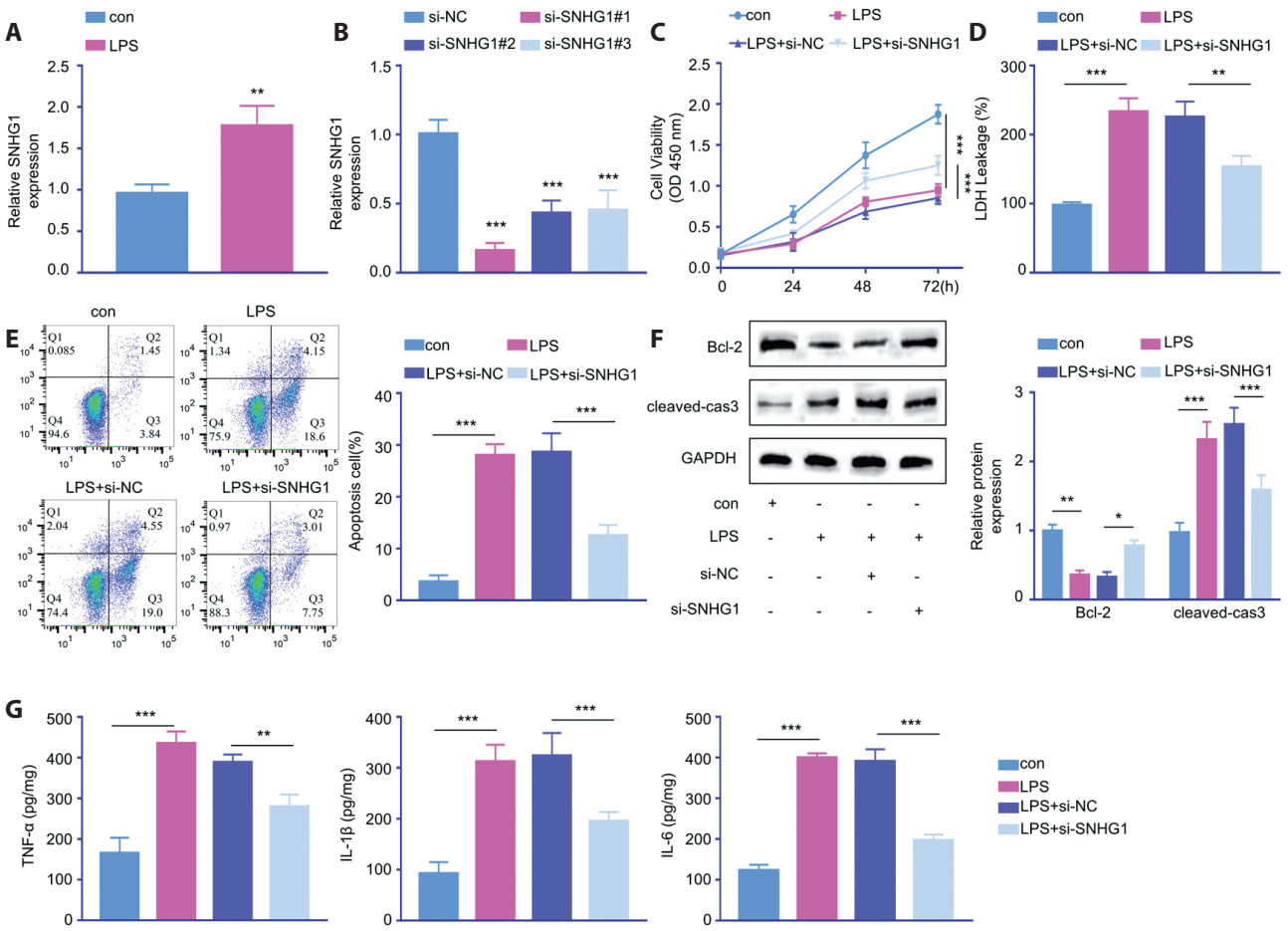

Figure 1. SNHG1 depletion attenuates LPS-induced cell injury in A549 cells. The RT-qPCR analysis presents the expression level of SNHG1 mRNA after LPS stimulation (**A**) or si-SNHG1 transfection (**B**). **C.** CCK-8 assay determines cell proliferation ability. **D.** LDH assay determines its leakage level (cytotoxicity) in the cell culture medium. **E.** FACS analysis of apoptotic events by Annexin V and PI staining. **F.** Western blot analysis presents the expression levels of Bcl-2 and cleaved caspase-3 proteins. **G.** ELISA assay determines the intracellularly generated TNF-α, IL-1β , and IL-6 levels in a cell culture medium. Data are presented as mean ± SD from 3 independent experiments; ** $p < 0.01$, *** $p < 0.001$.

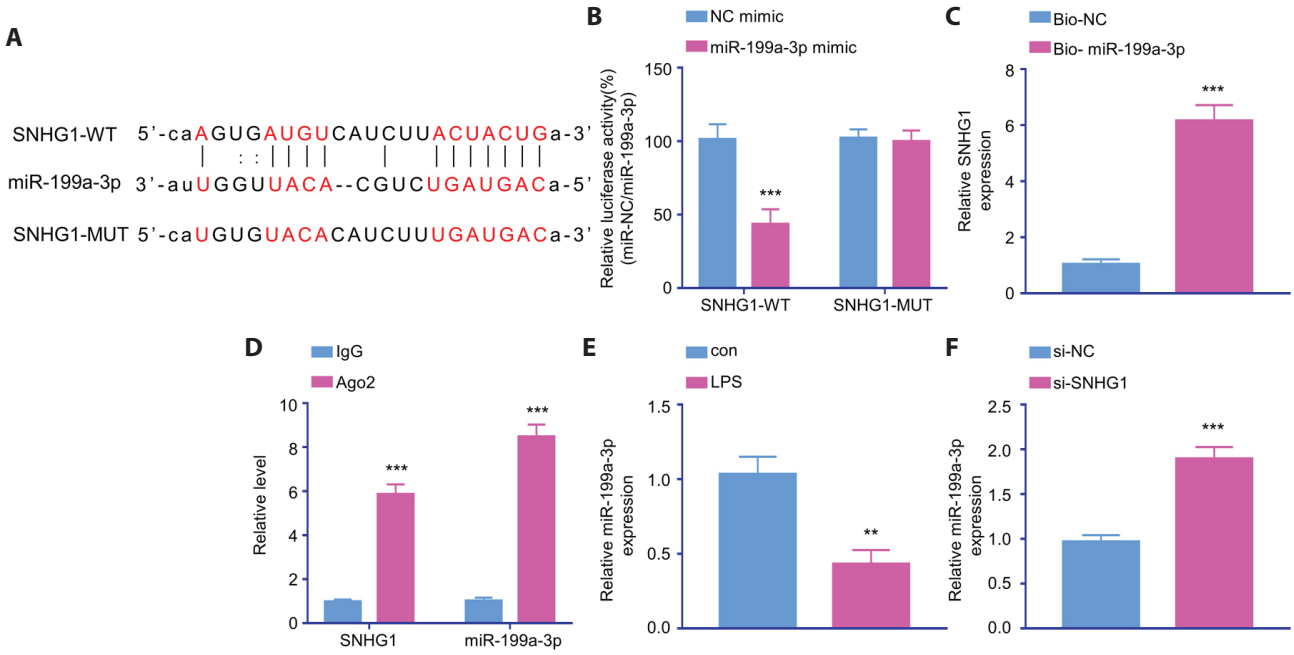

Figure 2. SNHG1 acts as a upstream regulator for miR-199a-3p in A549 cells. **A.** StarBase database predicts the binding sites between miR-199a-3p and SNHG1. **B.** The Dual-luciferase assay presents the relative luciferase activity of wild-type and mutant SNHG1 reporter in the transfected A549 cells with or without miR-199a-3p mimic. **C.** Biotinylated miR-199a-3p or NC probe is transfected into A549 cells, and an RNA pulldown assay is performed to assess the enrichment of SNHG1. **D.** The RIP assay determines the association of SNHG1 and miR-199a-3p with Ago2 protein. **E.,F.** RT-qPCR analysis measures miR-199a-3p mRNA levels. Data are presented as mean ± SD from 3 independent experiments; ** $p < 0.01$; *** $p < 0.001$.

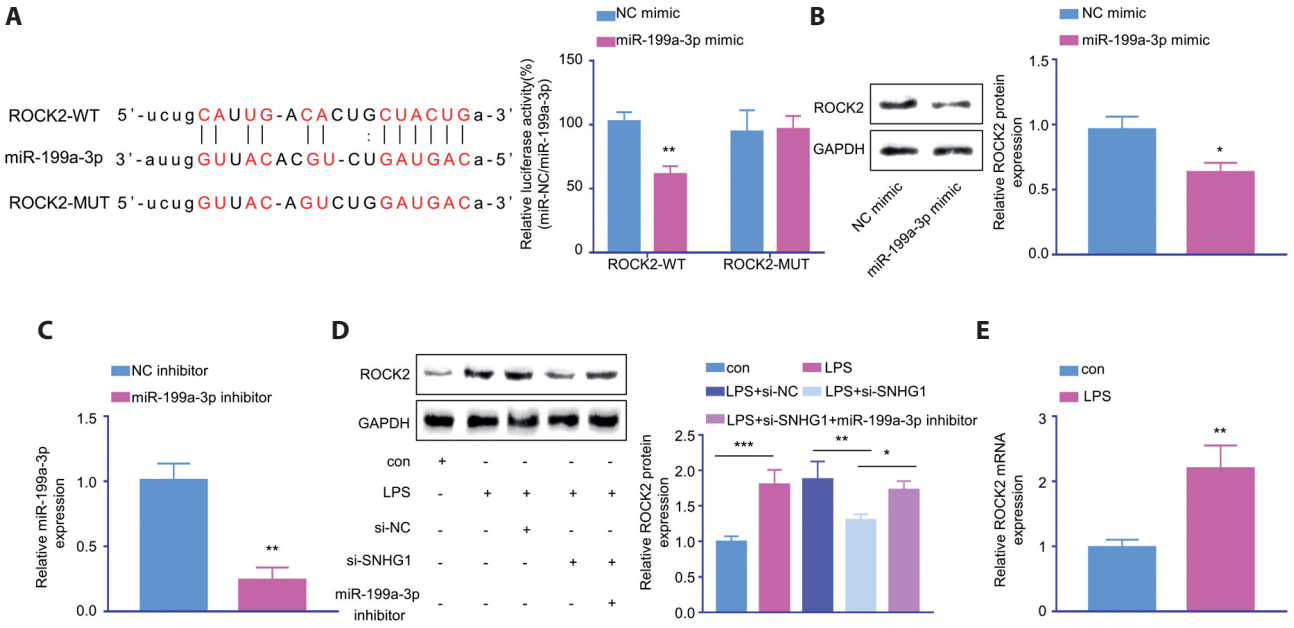

Figure 3. SNHG1 modulates ROCK2 expression by targeting miR-199a-3p. **A.** StarBase analysis predicts the binding sites between miR-199a-3p and ROCK2. The dual-luciferase assay measures the relative luciferase activity of wild-type, or mutant reporter with or without miR-199a-3p mimic co-transfection. **B.** Western blot analysis measures ROCK2 protein levels after miR-199a-3p mimic transfection. **C.** RT-qPCR analysis determines miR-199a-3p mRNA level. Western blot (**D**) and RT-qPCR (**E**) analyses determine ROCK2 expression levels in each experimental group. Data are presented as mean ± SD from 3 independent experiments; ** $p < 0.01$; *** $p < 0.001$.

SNHG1 modulates ROCK2 expression by targeting miR-199a-3p

Furthermore, we investigated the role of miR199a-3p in LPS-induced A549 cells. Utilizing StarBase software, we identified potential binding sites between miR199a-3p and ROCK2 mRNA. Subsequent dual-luciferase reporter assays confirmed reduced luciferase activity upon miR199a-3p transfection in the reporter containing wild type ROCK2 binding sites, while no change was observed in the mutated reporter (Fig. 3A). Immunoblotting results further demonstrated decreased ROCK2 expression with miR199a-3p overexpression (Fig. 3B). We performed additional validation using miR-199a-3p inhibitor which could effectively reduce miR-199a-3p levels (Fig. 3C). We observed that LPS induction elevated the protein level of ROCK2, and SNHG1 knockdown reversed this effect. However, the introduction of miR-199a-3p inhibitor abrogated the effect of SNHG1 knockdown (Fig. 3D,E). These findings suggest that SNHG1 functions as a molecular inhibitor of miR-199a-3p in the regulation of ROCK2 expression.

SNHG1 regulates LPS-induced A549 cell injury via miR-199a-3p/ROCK2 axis

To further confirm the involvement of miR-199a-3p/ROCK2 axis in regulating LPS-induced cell injury, A549 cells were transfected with SNHG1 siRNA alone or in combination with miR-199a-3p inhibitor or ROCK2 overexpressing plasmid. Western blot analysis demonstrated that the ROCK2 overexpressing plasmid effectively increased ROCK2 expression (Fig. 4A). CCK-8 proliferation and LDH cytotoxicity assay demonstrated that SNHG1 knockdown significantly rescued LPS-induced cellgrowth arrest and cell death, an effect that was partially reversed by miR-199a-3p inhibition or ROCK2 overexpression (Fig. 4B,C). Flow cytometry analysis revealed that SNHG1 knockdown suppressed cellular apoptosis under LPS stimulation (Fig. 4D). This was supported by reduced levels of cleaved caspase-3 and increased Bcl-2 expression in LPS-treated A549 cells upon SNHG1 depletion (Fig. 4E). Additionally, SNHG1 knockdown decreased TNF-α, IL-1β, and IL-6 expression in LPS-induced A549 cells (Fig.

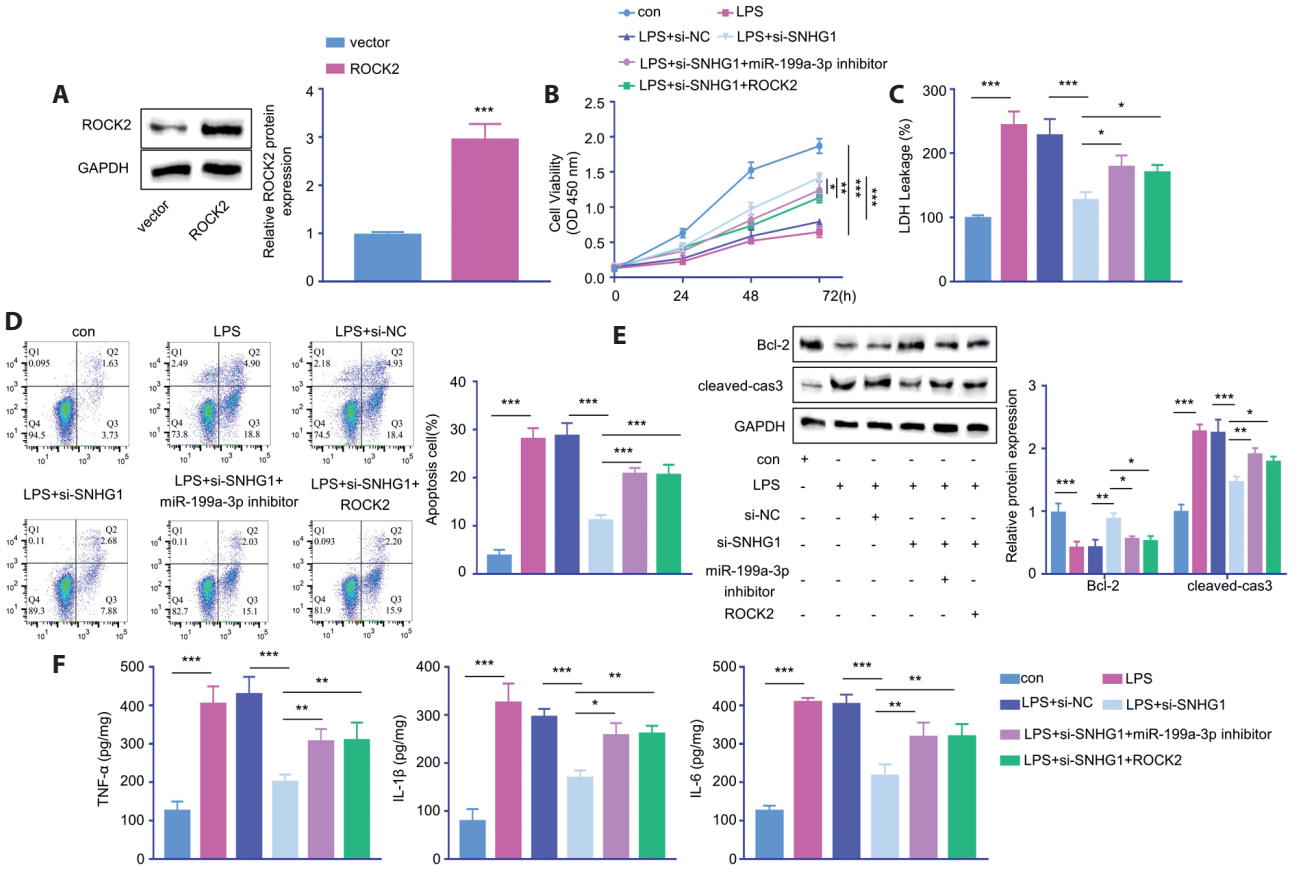

Figure 4. SNHG1 impinges on LPS-induced A549 cell injury *via* miR199a-3p/ROCK2 axis. **A.** Western blot analysis presents the expression levels of ROCK2 protein. **B.** The CCK-8 assay determines A549 cell proliferation rate. **C.** LDH cytotoxicity assay. **D.** FACS analysis of cell apoptosis rate. **E.** Western blot determination of Bcl-2 and cleaved caspase-3 protein levels. **F.** ELISA presents the expression levels of TNF-α, IL-1β, and IL-6 levels in cell culture medium. Data are presented as mean ± SD from 3 independent experiments; * $p < 0.05$;** $p < 0.01$; *** $p < 0.001$.

4F). These effects were curtailed by forced ROCK2 expression or miR-199a-3p suppression (Fig. 4D–F). Overall, the findings strongly suggest that SNHG1 silencing mitigates LPS-induced A549 cell injury through the miR-199a-3p/ROCK2 axis.

SNHG1 silencing alleviates LPS-induced inflammation and injury in vivo

Following the observed effects of SNHG1 in A549 cells *in vitro*, the adeno-associated virus carrying SNHG1 shRNA (AAV-sh-SNHG1) was developed to silence SNHG1 *in vivo,* with AAV-NC serving as the control. Histological analysis revealed that LPS stimulation led to increased lung tissue damage and injury scores in mice. Interestingly, AAV-sh-SNHG1 treatment significantly mitigated the pathological changes induced by LPS injury (Fig. 5A). Additionally, LPS exposure resulted in a higher wet-to-dry mass ratio in isolated lungs, whereas AAV-sh-SNHG1 administration reduced this ratio, indicating a reduction in pulmonary edema (Fig. 5B). Subsequent TUNEL assay demonstrated that LPS injection increased apoptosis in the mouse model, while AAV-sh-SNHG1 treatment notably suppressed the apoptosis rate (Fig. 5C). Furthermore, silencing SNHG1 prevented the upregulation of inflammatory factors in lung tissues of LPS-treated mice (Fig. 5D).

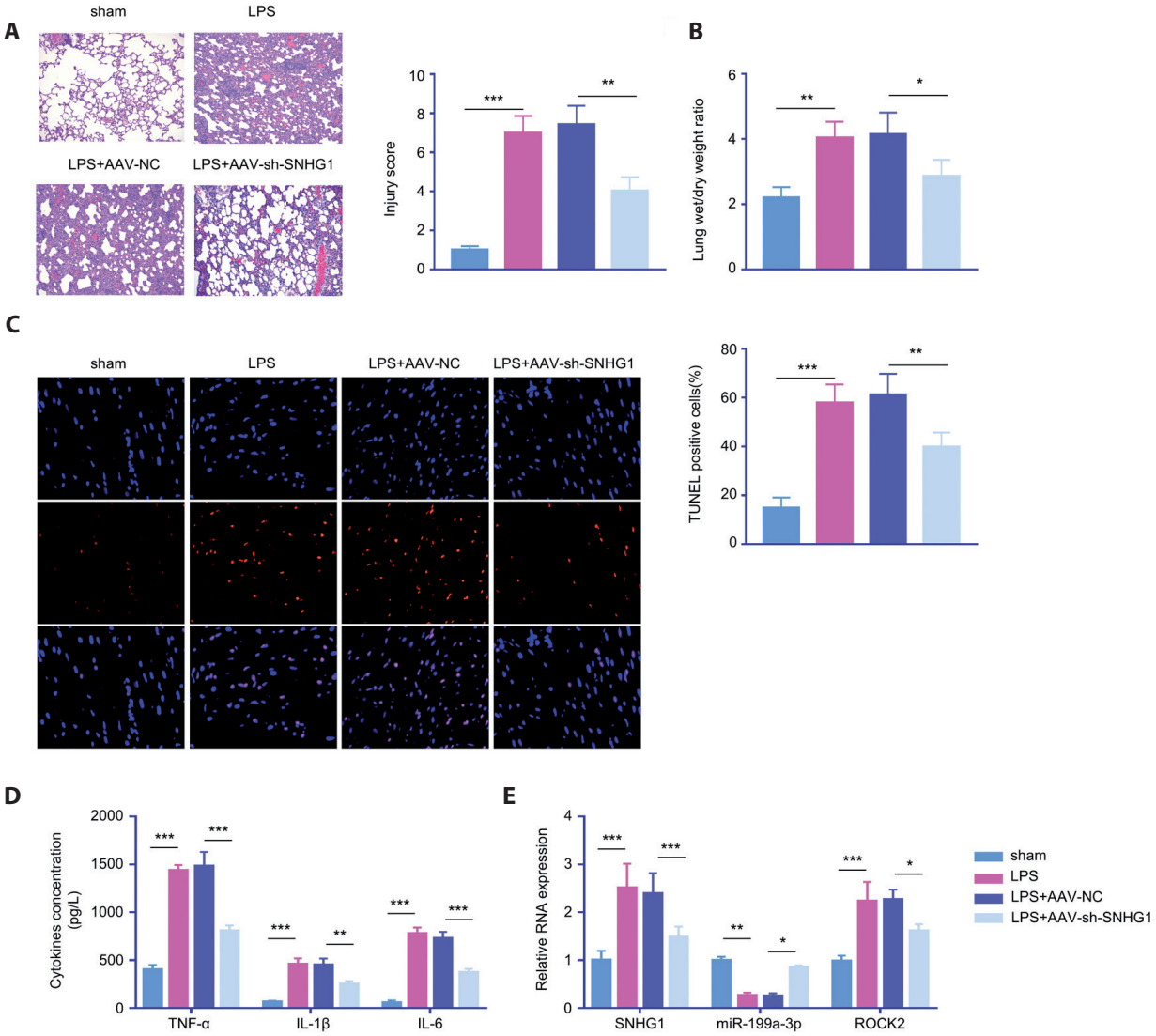

Figure 5. SNHG1 knockdown alleviates LPS-induced inflammation and injury *in vivo*. **A.** H&E staining of lung tissues sections after different treatments (magnification ×100). **B.** Summary of wet/dry ratio of lung tissues in each group. **C.** TUNEL assay of apoptotic events in lung tissue section. **D.** ELISA measurement of of TNF-α, IL-6, and IL-1β in BALF samples. **E.** RT-qPCR analysis of SNHG1, miR199a-3p, and ROCK2 expression levels in lung tissues. $n = 8$ animals *per* group; * $p < 0.05$; ** $p < 0.01$; *** $p < 0.001$.

Moreover, AAV-sh-SNHG1 administration suppressed the expression levels of SNHG1 and ROCK2, while restored miR-199a-3p expression in LPS-treated lung tissues (Fig. 5E). Collectively, these findings indicate that SNHG1 silencing could serve as strategy to alleviates LPS-induced acute lung injury *in vivo*.

Discussion

The present study demonstrated that SNHG1 depletion attenuated LPS-induced cell injury, apoptosis, and inflammation in A549 cells. Mechanistically, SNHG1 acted as a molecular inhibitor for miR-199a-3p, thereby regulating the expression of ROCK2. The protective effects of SNHG1 silencing against LPS-induced cell injury were mediated through the miR-199a-3p/ROCK2 axis. Furthermore, *in vivo* experiments revealed that SNHG1 deficiency alleviated LPS-induced inflammation and lung injury in mice. These findings provide novel insights into the role of SNHG1 in the pathogenesis of ALI and suggest its potential as a therapeutic target.

Previous studies have reported the involvement of lncRNA SNHG1 in regulating apoptosis and inflammation in various cell types and disease models. For instance, SNHG1 has been shown to promote apoptosis and inflammation in osteoarthritis by targeting the miR-16-5p/SMAD7 axis (Wang et al. 2024). Similarly, SNHG1 knockdown attenuated neuronal apoptosis and inflammation in ischemic stroke by targeting the miR-18a-5p/KLF4 axis (Zhang et al. 2020). These findings were consistent with our observation that SNHG1 knockdown exerted protective effects against LPS-induced apoptosis and inflammation in ALI model.

Nevertheless, SNHG1 has been reported as an oncogenic factor to promote tumor progression. SNHG1 overexpression enhances the malignancy of breast cancer cells by regulating miR-382 and epithelial-to-mesenchymal transition (Zheng et al. 2019). Moreover, SNHG1 promotes osteosarcoma progression by inhibiting miR-101-3p activity and activating the Wnt/β-catenin pathway (Jiang et al. 2018). SNHG1 upregulation is correlated with poor patient prognosis and exerts anti-apoptotic effects in hepatocellular carcinoma and colorectal cancer (Zhang et al. 2016; Zhu et al. 2017) These studies highlight the complex and context-dependent roles of SNHG1 in apoptosis. Nevertheless, the divergent roles of SNHG1 may be attributed to differences in the intracellular environment and the availability of specific target molecules in distinct cell types and tissues.

The contrasting effects of SNHG1 on cellular processes, such as apoptosis regulation, may be attributed to the specific intracellular environment and the repertoire of miRNAs present in distinct cell or tissue types. LncRNAs, including SNHG1, can act as molecular regulators for various miRNAs, thereby modulating the expression of their target genes. In the present study, we identified miR-199a-3p as a direct target of SNHG1 in A549 cells. Depletion of miR-199a-3p abolished the protective effects of SNHG1 knockdown on LPS-induced apoptosis and inflammation. Notably, miR-199a-3p has been reported to play a crucial role in ALI pathogenesis, as well as in other inflammatory diseases (Wangyang et al. 2018; Chen et al. 2019; Yang et al. 2019; Li et al. 2020; Xu et al. 2022; Zhang et al. 2022). The anti-inflammatory and anti-apoptotic effects of miR-199a-3p observed in this study are consistent with previous findings in various disease models. For instance, downregulation of miR-199a-3p in alveolar macrophages exacerbated LPS-induced acute respiratory distress syndrome (ARDS) by promoting the release of pro-inflammatory secretory autophagosomes (Xu et al. 2022). Similarly, downregulation of miR-199a-3p contributed to acute lung injury by targeting NLRP1, a component of the inflammasome complex (Chen et al. 2019). The anti-apoptotic effects of miR-199a-3p are also supported by studies in other contexts. For example, miR-199a-3p inhibited hepatic apoptosis and hepatocarcinogenesis by targeting the pro-apoptotic gene PDCD4 (Liu et al. 2020), while miR-199a-3p suppressed high glucose-induced apoptosis in renal tubular epithelial cells (Zhang et al. 2022).

In our study, we further identified ROCK2 as a direct downstream target of miR-199a-3p. ROCK2 is a serine-threonine kinase that has been implicated in various cellular processes, including inflammation, apoptosis, cytoskeletal reorganization, and cell migration (Johan et al. 2019). Notably, ROCK2 has been reported to be upregulated in ALI, contributing to the pathogenesis of the disease (Chen et al. 2020; Ren et al. 2022). ROCK2 activation has been associated with increased inflammation, oxidative stress, and endothelial dysfunction (Qian et al. 2022; Glotfelty et al. 2023). Furthermore, ROCK2 inhibition has been shown to attenuate LPS-induced lung injury by reducing inflammatory cytokine production, neutrophil infiltration, and vascular leakage (Rodriguez-Pineiro et al. 2023). In addition, ROCK2 has been implicated in the regulation of apoptosis in various cell types, such as endothelial cells and cardiomyocytes (Shi et al. 2007; Hartmann et al. 2015), suggesting its diverse roles in different cellular contexts. By acting as a negative regulator for miR-199a-3p, SNHG1 promoted the expression of ROCK2, thereby exacerbating LPS-induced cell injury and inflammation in A549 cells. Importantly, the protective effects of SNHG1 silencing against LPS-induced cell injury were abrogated by miR-199a-3p inhibition or ROCK2 overexpression, further validating the involvement of the miR-199a-3p/ROCK2 axis in the regulatory mechanisms of SNHG1.

Consistent with our *in vitro* findings, we demonstrated that SNHG1 knockdown attenuates LPS-induced lung in-

jury, apoptosis, and inflammation in a mouse model of ALI. These results provide strong evidence for the therapeutic potential of targeting SNHG1 in the treatment of ALI. However, further studies are needed to evaluate the safety and efficacy of SNHG1-targeted therapies in preclinical models and to explore the potential for clinical translation.

Conclusion

In conclusion, our findings revealed that SNHG1 knockdown attenuated LPS-induced acute lung injury by regulating the miR-199a-3p/ROCK2 axis, providing new insights into the pathogenesis of ALI and potential therapeutic targets. However, it is important to note that the miRNA environment in different cell types may influence the functional roles of lncRNAs, such as SNHG1. Further studies are warranted to elucidate the cell-type-specific miRNA networks and their interplay with lncRNAs in the context of ALI and other inflammatory disorders.

Declaration ethical approval. All animal-related experiments and their detailed procedures were approved by the Second Hospital of Dalian Medical University Animal Policy and Welfare Committee.

Authors contributions. Yan Jin designed the study and wrote the first draft of the manuscript and conducted the statistical analysis. Yan Jin performed the data collection and took part in statistical analysis. Xue Lin provided critical input into the data analysis and interpretation of the results. Xue Lin participated in conception, designed of the study and revised it critically for important intellectual content. All authors have read the draft critically to make contributions and also approved the final manuscript.

Conflict of interest. The authors declare that they have no competing interests.

Availability of data and materials. The data is available upon reasonable request.

References

Cai ZG, Zhang SM, Zhang Y, Zhou YY, Wu HB, Xu XP (2012): MicroRNAs are dynamically regulated and play an important role in LPS-induced lung injury. Can. J. Physiol. Pharmacol. **90,** 37-43
https://doi.org/10.1139/y11-095

Chen H, Hu X, Li R, Liu B, Zheng X, Fang Z, Chen L, Chen W, Min L, Hu S (2020): LncRNA THRIL aggravates sepsis-induced acute lung injury by regulating miR-424/ROCK2 axis. Mol. Immunol. **126,** 111-119
https://doi.org/10.1016/j.molimm.2020.07.021

Chen L, Hou Y, Du D, Cui Y, Nie H, Ding Y (2022): MiR-199a-3p in mouse bone marrow mesenchymal stem cell exosomes increases epithelial sodium channel expression in lung injury. Fundam. Clin. Pharmacol. **36,** 1011-1019
https://doi.org/10.1111/fcp.12807

Chen Z, Dong WH, Chen Q, Li QG, Qiu ZM (2019): Downregulation of miR-199a-3p mediated by the CtBP2-HDAC1-FOXP3 transcriptional complex contributes to acute lung injury by targeting NLRP1. Int. J. Biol. Sci. **15,** 2627-2640
https://doi.org/10.7150/ijbs.37133

Fatica A, Bozzoni I (2014): Long non-coding RNAs: new players in cell differentiation and development. Nat. Rev. Genet. **15,** 7-21
https://doi.org/10.1038/nrg3606

Gantier MP (2010): New perspectives in microRNA regulation of innate immunity. J. Interferon Cytokine Res. **30,** 283-289
https://doi.org/10.1089/jir.2010.0037

Glotfelty EJ, Tovar YRLB, Hsueh SC, Tweedie D, Li Y, Harvey BK, Hoffer BJ, Karlsson TE, Olson L, Greig NH (2023): The RhoA-ROCK1/ROCK2 pathway exacerbates inflammatory signaling in immortalized and primary microglia. Cells **12,** 1367
https://doi.org/10.3390/cells12101367

Hartmann S, Ridley AJ, Lutz S (2015): The function of Rho-associated kinases ROCK1 and ROCK2 in the pathogenesis of cardiovascular disease. Front. Pharmacol. **6,** 276
https://doi.org/10.3389/fphar.2015.00276

Hu C, Li J, Tan Y, Liu Y, Bai C, Gao J, Zhao S, Yao M, Lu X, Qiu L, et al. (2022): Tanreqing injection attenuates macrophage activation and the inflammatory response via the lncRNA-SNHG1/HMGB1 axis in lipopolysaccharide-induced acute lung injury. Front. Immunol. **13,** 820718
https://doi.org/10.3389/fimmu.2022.820718

Jiang Z, Jiang C, Fang J (2018): Up-regulated lnc-SNHG1 contributes to osteosarcoma progression through sequestration of miR-577 and activation of WNT2B/Wnt/beta-catenin pathway. Biochem. Biophys. Res. Commun. **495,** 238-245
https://doi.org/10.1016/j.bbrc.2017.11.012

Johan MZ, Samuel MS (2019): Rho-ROCK signaling regulates tumor-microenvironment interactions. Biochem. Soc. Trans. **47,** 101-108
https://doi.org/10.1042/BST20180334

Li W, Dong X, He C, Tan G, Li Z, Zhai B, Feng J, Jiang X, Liu C, Jiang H, et al. (2019): LncRNA SNHG1 contributes to sorafenib resistance by activating the Akt pathway and is positively regulated by miR-21 in hepatocellular carcinoma cells. J. Exp. Clin. Cancer Res. **38,** 183
https://doi.org/10.1186/s13046-019-1177-0

Li Z, Zhou Y, Zhang L, Jia K, Wang S, Wang M, Li N, Yu Y, Cao X, Hou J (2020): microRNA-199a-3p inhibits hepatic apoptosis and hepatocarcinogenesis by targeting PDCD4. Oncogenesis **9,** 95
https://doi.org/10.1038/s41389-020-00282-y

Liu L, Shi Y, Shi J, Wang H, Sheng Y, Jiang Q, Chen H, Li X, Dong J (2019): The long non-coding RNA SNHG1 promotes glioma progression by competitively binding to miR-194 to regulate PHLDA1 expression. Cell Death Dis. **10,** 463
https://doi.org/10.1038/s41419-019-1698-7

Liu Y, Guan H, Zhang JL, Zheng Z, Wang HT, Tao K, Han SC, Su LL, Hu D (2018): Acute downregulation of miR-199a attenuates sepsis-induced acute lung injury by targeting SIRT1. Am. J. Physiol. Cell Physiol. **314,** C449-C455

https://doi.org/10.1152/ajpcell.00173.2017
Liu ZQ, He WF, Wu YJ, Zhao SL, Wang L, Ouyang YY, Tang SY (2020): LncRNA SNHG1 promotes EMT process in gastric cancer cells through regulation of the miR-15b/DCLK1/Notch1 axis. BMC Gastroenterol. **20,** 156
https://doi.org/10.1186/s12876-020-01272-5
Lv S, Qu X, Qu Y, Wang Y (2021): LncRNA NEAT1 knockdown alleviates lipopolysaccharide-induced acute lung injury by modulation of miR-182-5p/WISP1 axis. Biochem. Genet. **59,** 1631-1647
https://doi.org/10.1007/s10528-021-10081-8
Mercer TR, Dinger ME, Mattick JS (2009): Long non-coding RNAs: insights into functions. Nat. Rev. Genet. **10,** 155-159
https://doi.org/10.1038/nrg2521
Mowery NT, Terzian WTH, Nelson AC (2020): Acute lung injury. Curr. Probl. Surg. **57,** 100777
https://doi.org/10.1016/j.cpsurg.2020.100777
Qian X, Yang L (2022): ROCK2 knockdown alleviates LPS-induced inflammatory injury and apoptosis of renal tubular epithelial cells via the NF-kappaB/NLRP3 signaling pathway. Exp. Ther. Med. **24,** 603
https://doi.org/10.3892/etm.2022.11540
Qiu N, Xu X, He Y (2020): LncRNA TUG1 alleviates sepsis-induced acute lung injury by targeting miR-34b-5p/GAB1. BMC Pulm. Med. **20,** 49
https://doi.org/10.1186/s12890-020-1084-3
Ren Y, Li L, Wang M, Yang Z, Sun Z, Zhang W, Cao L, Nie S (2022): Knockdown of circRNA paralemmin 2 ameliorates lipopolysaccharide-induced murine lung epithelial cell injury by sponging miR-330-5p to reduce ROCK2 expression. Immunol. Invest. **51,** 1707-1724
https://doi.org/10.1080/08820139.2022.2027961
Rodriguez-Pineiro AM, Jaudas F, Klymiuk N, Bahr A, Hansson GC, Ermund A (2023): Proteome of airway surface liquid and mucus in newborn wildtype and cystic fibrosis piglets. Respir. Res. **24,** 83
https://doi.org/10.1186/s12931-023-02381-x
Schmidt GA (2016): Managing acute lung injury. Clin. Chest Med. **37,** 647-658
https://doi.org/10.1016/j.ccm.2016.07.005
Shi J, Wei L (2007): Rho kinase in the regulation of cell death and survival. Arch. Immunol. Ther. Exp. (Warsz.) **55,** 61-75
https://doi.org/10.1007/s00005-007-0009-7
Wang Q, Yang J, Pan R, Zha Z (2024): LncRNA SNHG1 overexpression alleviates osteoarthritis via activating PI3K/Akt signal pathway and suppressing autophagy. Immunobiology **229,** 152799
https://doi.org/10.1016/j.imbio.2024.152799
Wang Y, Yang W, Zhao X, Zhang R (2018): Experimental study of the protective effect of simvastatin on lung injury in rats with sepsis. Inflammation **41,** 104-113
https://doi.org/10.1007/s10753-017-0668-4
Wangyang Y, Yi L, Wang T, Feng Y, Liu G, Li D, Zheng X (2018): MiR-199a-3p inhibits proliferation and induces apoptosis in rheumatoid arthritis fibroblast-like synoviocytes via suppressing retinoblastoma 1. Biosci. Rep. **38,** BSR20180982
https://doi.org/10.1042/BSR20180982
Xu J, Yang R, Hua X, Huang M, Tian Z, Li J, Lam HY, Jiang G, Cohen M, Huang C (2020): lncRNA SNHG1 promotes basal bladder cancer invasion via interaction with PP2A catalytic subunit and induction of autophagy. Mol. Ther. Nucleic Acids **21,** 354-366
https://doi.org/10.1016/j.omtn.2020.06.010
Xu X, Liu X, Dong X, Yang Y, Liu L (2022): MiR-199a-3p-regulated alveolar macrophage-derived secretory autophagosomes exacerbate lipopolysaccharide-induced acute respiratory distress syndrome. Front. Cell. Infect. Microbiol. **12,** 1061790
https://doi.org/10.3389/fcimb.2022.1061790
Yang A, Liu F, Guan B, Luo Z, Lin J, Fang W, Liu L, Zuo W (2019): p53 induces miR-199a-3p to suppress mechanistic target of rapamycin activation in cisplatin-induced acute kidney injury. J. Cell. Biochem. **120,** 17625-17634
https://doi.org/10.1002/jcb.29030
Zhang M, Wang W, Li T, Yu X, Zhu Y, Ding F, Li D, Yang T (2016): Long noncoding RNA SNHG1 predicts a poor prognosis and promotes hepatocellular carcinoma tumorigenesis. Biomed. Pharmacother. **80,** 73-79
https://doi.org/10.1016/j.biopha.2016.02.036
Zhang R, Qin L, Shi J (2020): MicroRNA-199a-3p suppresses high glucose-induced apoptosis and inflammation by regulating the IKKbeta/NF-kappaB signaling pathway in renal tubular epithelial cells. Int. J. Mol. Med. **46,** 2161-2171
https://doi.org/10.3892/ijmm.2020.4751
Zhang R, Niu Z, Liu J, Dang X, Feng H, Sun J, Pan L, Peng Z (2022): LncRNA SNHG1 promotes sepsis-induced myocardial injury by inhibiting Bcl-2 expression via DNMT1. J. Cell. Mol. Med. **26,** 3648-3658
https://doi.org/10.1111/jcmm.17358
Zheng S, Li M, Miao K, Xu H (2019): SNHG1 contributes to proliferation and invasion by regulating miR-382 in breast cancer. Cancer Manag. Res. **11,** 5589-5598
https://doi.org/10.2147/CMAR.S198624
Zhu Y, Li B, Liu Z, Jiang L, Wang G, Lv M, Li D (2017): Upregulation of lncRNA SNHG1 indicates poor prognosis and promotes cell proliferation and metastasis of colorectal cancer by activation of the Wnt/beta-catenin signaling pathway. Oncotarget **8,** 111715-111727
https://doi.org/10.18632/oncotarget.22903

Received: February 16, 2024
Final version accepted: April 9, 2024